THE ANATOMICAL RECORD 296:1264–1282 (2013)

How Effective Are Geometric Morphometric Techniques for Assessing Functional Shape Variation? An Example From the Great Ape Temporomandibular Joint

CLAIRE E. TERHUNE*
Department of Community and Family Medicine, Duke University Medical Center,
Durham, North Carolina

ABSTRACT

Functional shape analyses have long relied on the use of shape ratios to test biomechanical hypotheses. This method is powerful because of the ease with which results are interpreted, but these techniques fall short in quantifying complex morphologies that may not have a strong biomechanical foundation but may still be functionally informative. In contrast, geometric morphometric methods are continually being adopted for quantifying complex shapes, but they tend to prove inadequate in functional analyses because they have little foundation in an explicit biomechanical framework. The goal of this study was to evaluate the intersection of these two methods using the great ape temporomandibular joint as a case study. Three-dimensional coordinates of glenoid fossa and mandibular condyle shape were collected using a Microscribe digitizer. Linear distances extracted from these landmarks were analyzed using a series of one-way ANOVAs; further, the landmark configurations were analyzed using geometric morphometric techniques. Results suggest that the two methods are broadly similar, although the geometric morphometric data allow for the identification of shape differences among taxa that were not immediately apparent in the univariate analyses. Furthermore, this study suggests several new approaches for translating these shape data into a biomechanical context by adjusting the data using a biomechanically relevant variable. Anat Rec, 296:1264–1282, 2013. © 2013 Wiley Periodicals, Inc.

Key words: geometric morphometrics; masticatory biomechanics; size and scaling

Biomechanical analyses seeking to quantify and compare morphological variation among species may take many forms. These functional shape analyses typically assess specific morphological features predicted to vary by theoretical models, or they expand upon experimental studies that have previously identified functionally significant features (e.g., Hylander, 1975, 1979; Greaves, 1978; Smith, 1978; Hylander and Bays, 1979; Bouvier, 1986a,b;

Grant sponsor: National Science Foundation Doctoral Dissertation Grant, the Leakey Foundation; Grant number: NSF BCS-0752661.

*Correspondence to: Claire E. Terhune; Department of Community and Family Medicine, Duke University Medical Center, Box 104780, Durham, NC 27710. Fax: (919)-684-1846.
E-mail: claire.terhune@duke.edu

Received 9 January 2013; Accepted 28 April 2013.
DOI 10.1002/ar.22724

Antón, 1996; Wall, 1999; Daegling and McGraw, 2001; Vinyard et al., 2003; Taylor, 2005, 2006; Norconk et al., 2009). These analyses are primarily restricted to evaluating discrete features and they rely on the use of scaling variables that have some biomechanical significance for the shape under investigation (Jungers, 1984; Hylander, 1985; Bouvier, 1986a,b; Smith, 1993; Vinyard, 2008). These methods are powerful because of their ease of interpretation in the context of biomechanical models, but they are not as well equipped for evaluating functional shape variation in complex morphological features.

In contrast, geometric morphometric (GM) techniques for analyzing shape variation have gained considerable popularity over the last 20 years and are now widely employed in many disciplines (e.g., Lynch et al., 1996; O'Higgins and Jones, 1998; Adams and Rohlf, 2000; Klingenberg et al., 2001; Lockwood et al., 2002, 2004; Adams, 2004; Bonnan, 2007; Pierce et al., 2008; Brusatte et al., 2012). These methodologies, which use two- or three-dimensional coordinates (2D and 3D, respectively) to capture shape, are excellent at summarizing shape variation in entire configurations of coordinates both among and within operational units. The chief use of this methodology is often to explore and describe intra- and interspecific shape variation (e.g., Lockwood et al., 2002; Harvati, 2003; Smith et al., 2007; Gunz et al., 2009), and the adoption of these methods has led to the development and refinement of techniques that allow for the analysis of size-related shape variation (e.g., Viðarsdottir et al., 2002; Mitteroecker et al., 2004; Baab and McNulty, 2009), covariance in and among structures (Bookstein et al., 1999, 2003; Klingenberg, 2009), and many others. However, the utility of geometric morphometric methods for analyses specifically designed to assess biomechanical variation has lagged behind.

The goal of this study is to compare and contrast these two distinct methodologies, with the ultimate goal of proposing ways in which these methods may be combined to more effectively evaluate shape variation in a biomechanical context. Although there are a number of ways in which these methods may differ, I focus here on two specific differences: (1) considerations of size and scaling; and (2) univariate vs. multivariate shape analysis.

SIZE AND SCALING

Functional shape analyses typically employ either body size or a geometric mean of the features being examined as a scaling variable (e.g., Smith et al., 1983; Jungers, 1984; Dumont, 1997; Lewton, 2012; and others). In studies analyzing components of the locomotory system, or when the focus of the research is the relationship to body mass (e.g., as an indicator of metabolic demands), these variables are appropriate. However, as argued by Hylander (1985), biomechanical analyses of the facial skeleton do not benefit from the exclusive use of body mass, since "primates do not routinely transmit body weight or locomotor stress through their faces" (Hylander, 1985:325). Thus, in the masticatory literature mandible length, which serves as an estimate of the bite force lever arm during incision (Hylander, 1985; Bouvier, 1986a,b; Vinyard et al., 2003; Vinyard, 2008), has become the preferred scaling variable. Some authors have also used the distance from the mandibular condyle to the first molar (TMJ-M_1) as a measure of the lever arm during postcanine masticatory behaviors (e.g., Ravosa, 1990; Taylor, 2006). In either case, analyses using these biomechanically relevant variables can differ substantially from those where estimates of overall cranial or body size are employed (Vinyard, 2008). Thus, the measure of size against which features are evaluated may substantially influence the outcome and interpretation of the analysis.

Size data are commonly used in two ways in traditional morphometric analyses. First, when the goal of the analysis is to evaluate differences among taxa, size is often "accounted for" by the creation of shape ratios that divide the feature in question by a relevant size variable, or through the use of residuals where the feature being examined is regressed on a size variable and the regression residuals extracted for further analysis (see Jungers et al. [1995] and Smith (2005) for detailed reviews of these and other methods). Both of these techniques (and particularly the former) allow for the analysis of relative shape differences among taxa. Second, analyses focusing on functional scaling patterns must also necessarily utilize a size variable; these analyses classically regress a variable of interest (e.g., molar area) on a relevant size variable (e.g., body mass) to examine whether the scaling relationship between these two variables is positively or negatively allometric, or isometric in nature (e.g., Vinyard and Hanna, 2005).

The treatment of size in GM differs from that of traditional morphometric analyses. The first step in most GM analyses is superimposition, which translates, rotates, and scales all landmark configurations such that only shape remains. During this process, all specimens are scaled to unit centroid size (defined as the square root of the sum of squared distances from each landmark to the centroid of the landmark configuration; Zelditch et al., 2004), and the centroid size of each specimen is extracted as a separate variable. Centroid size can then be used in further analyses. However, it is important to note that, although size is held constant across landmark configurations, allometric shape differences remain; thus, regressions of the PC axes or Procrustes rotated coordinates (i.e., Procrustes residuals) on centroid size are powerful tools for indicating whether allometric shape variation exists within the sample. In many ways, the GM "removal" of size during superimposition is similar to the creation of shape ratios discussed above; both analyses examine shape variation among specimens when size is held constant across specimens. However, the main difference between these approaches is the size variable with which shape variation is standardized. One major drawback to the approach taken by GM methods is that the centroid size of the configuration being examined is not necessarily biomechanically relevant. Examining shape variation in the sample as it relates to size of the configuration is therefore unlikely to be functionally meaningful.

UNIVARIATE VS. MULTIVARIATE SHAPE ANALYSIS

Biomechanical hypotheses are often framed to examine features in isolation from one another. For example, measures of joint width are typically not also able to describe joint convexity; instead, these two measures would be quantified separately. These analyses therefore highlight specific features which vary in functional predictable ways (e.g., relative to a specific lever arm or body mass). However, functional shape ratios sometimes limit our inferences regarding shape variation. For example, mandibular condylar width and curvature may both be of interest for evaluating joint loading and range of motion at the temporomandibular joint, but these two variables would most commonly be examined separately. Although when multiple variables are included in the same study the general pattern of shape differences among species may be apparent (e.g., species X has both a long and curved condyle), the overall form of the specimen or species being examined is lost by atomizing the morphology in this way. In other words, by breaking down shape into its component parts, we often lose the ability to assess how those parts may covary with one another. Furthermore, and perhaps more importantly, by targeting our analyses to specific components of the morphology in question we limit the extent to which we can make novel observations about shape.

Geometric morphometric analyses are well known for their ability to quantify complex morphologies. However, this ability to examine multiple features in a single analysis also makes it difficult to place this shape variation in a biomechanical framework and to test hypotheses that are explicitly functional in nature. This difficulty results from the inclusion of multiple additional aspects of shape that may or may not covary with other aspects of the morphology being examined, and which may or may not have functional significance. One way to partly overcome this difficulty is for researchers to carefully consider the functional significance of each landmark in their dataset and to target their analyses to just those regions that may be functionally informative. For example, analyses of the masticatory apparatus should attempt to only evaluate those features that are functionally significant (e.g., the mandible) while avoiding capturing the morphology of regions that may be part of other functional units in the skulls (e.g., orbital morphology). However, given the often complex interactions between different morphological regions this may not always be an easy task, and further consideration of other potential factors influencing the observed morphology is critical.

STUDY GOALS

The purpose of this investigation is to compare and contrast functional shape analyses and geometric morphometric techniques. I highlight the pros and cons of these techniques rather than advocate that one is superior to the other. Furthermore, I suggest novel ways in which we might adjust GM techniques to better address biomechanical hypotheses and/or to identify the ways we might revise our biomechanical hypotheses to be more amenable to GM methods.

To contrast these two techniques I examine functional shape variation in the temporomandibular joint (TMJ) of the great apes. I use this region of the skull as a case study for several reasons. First, the extensive use of GM in studies of great ape, hominin, and human cranial form (e.g., Lockwood et al., 2002, 2004; Harvati, 2003; Mitteroecker et al., 2004; Rosas and Bastir, 2004; Smith et al., 2007; Terhune et al., 2007; Baab, 2008; Baab and McNulty, 2009; Smith, 2009; von Cramon-Taubadel and Smith, 2012) makes analysis of this region particularly relevant to functional questions regarding the evolution of the masticatory apparatus in the human lineage. Perhaps more importantly, theoretical, experimental, and comparative data for the masticatory apparatus (e.g., Hylander, 1975, 1979; Greaves, 1978; Hylander and Bays, 1979; Bouvier, 1986a,b; Hylander et al., 1987; Spencer, 1998; Vinyard, 1999; Wall, 1999; Anderson et al., 2002; Komiyama et al., 2003; Vinyard et al., 2003; Wall et al., 2006), along with behavioral and food material property data for several great ape taxa (Badrian and Malenky, 1984; Watts, 1984; Williamson et al., 1990; Tutin and Fernandez, 1993; Malenky and Wrangham, 1994; Elgart-Berry, 2004; Fox et al., 2004; Vogel et al., 2008) allow for the formulation of specific predictions for how ape taxa may vary in their biomechanical abilities. Terhune (2013) recently summarized this previous research as it applies to the TMJ, and tested a series of biomechanical hypotheses using univariate data. In this previous study I specifically addressed two research questions: 1) can features of the great ape TMJ be predictably linked to variation in joint load resistance?; and 2) can features of the great ape TMJ be predictably linked to variation in joint range of motion ? Given previous behavioral and biomechanical data (see references above and details in Terhune [2013]), I predicted that taxa masticating more resistant foods (e.g., *Gorilla* and *Pongo* vs. *Pan*) would have larger and relatively wider condyles. Further, I predicted that taxa with increased gape requirements, as might be necessary for incisal behaviors or for placing and crushing small resistant foods on the posterior dentition (e.g., *Pongo* and *Pan*), would have relatively anteroposteriorly elongated TMJ articular surfaces. Results of this work suggested that great ape taxa do differ in TMJ shape, but this shape variation is primarily linked to facilitating joint range of motion rather than load resistance.

To further examine morphological variation in the great ape TMJ using geometric morphometrics, and to compare and contrast these methods with those employed in Terhune (2013), the present study investigated several interrelated research questions:

1. Do taxa differ significantly in TMJ shape when analyzed using GM methods?
2. Do the GM data reflect the same shape variation observed in the univariate data?
3. Are there additional aspects of TMJ form that exhibit significant variation among taxa?

MATERIALS AND METHODS

Three- dimensional coordinates describing glenoid fossa and mandibular condyle shape (Table 1, Fig. 1) were collected for females and males from eight great ape taxa (Table 2). Data were collected using a Microscribe G2X digitizer (Immersion Corp). The measured accuracy for the Microscribe G2X is ±0.23mm, and an analysis of intraobserver error for this dataset found an average error of ~0.03 mm for the skull and 0.04 mm for the mandible (Terhune, 2010).

Univariate Analyses

For the univariate analyses (presented fully in Terhune, 2013), linear measurements were extracted from

TABLE 1. Temporomandibular joint landmark definitions

Landmark number	Landmark description
Glenoid landmarks	
1	Most inferior point on entoglenoid process
2	Most inferior point on articular tubercle
3	Most inferior point on postglenoid process
4	Deepest point in mandibular fossa in sagittal plane of postglenoid process point
5	Most anterior point on the articular surface of the mandibular fossa
6	Most lateral point on the articular surface of the mandibular fossa at the end of the long axis of the articular eminence
7	Most lateral point on the surface of the articular eminence
8	Most medial point on the surface of the articular eminence
9	Most medial point on the articular surface of the mandibular fossa at the end of the long axis of the articular eminence
10	Midpoint of the crest of the articular eminence
11	Most anterior point on the articular surface of the mandibular fossa along a line perpendicular to the long axis of the articular eminence
12	Point on the posterior edge of the articular eminence along a line perpendicular to the long axis of the articular eminence
Condyle landmarks	
13	Most lateral point on the articular surface of the mandibular condyle
14	Most medial point on the articular surface of the mandibular condyle
15	Midpoint of line connecting the medial and lateral poles of the mandibular condyle
16	Most posterior point on the articular surface of the mandibular condyle at the midpoint of the mediolateral curve
17	Most anterior point on the mandibular condyle at the midpoint of the mediolateral curve

Semilandmarks describing anteroposterior condylar curvature we also collected on the articular surface of the condyle between landmarks 16 and 17.

the coordinate data using the programs MacMorph (Spencer and Spencer, 1993) and Rhino 3D (McNeel & Associates, 2008) and used to create traditional functional shape ratios. Three dimensional renderings of the articular surfaces of the glenoid and condyle were created by collecting a dense cloud of 3D landmarks describing each of these surfaces; articular surface area was calculated using these point clouds. Biomechanical shape ratios were created in one of two ways (Hylander, 1985; Taylor, 2006; Vinyard, 2008). Features predicted to be related to masticatory behaviors were adjusted by dividing by the distance from the mandibular condyle to M_1 (as a measure of the load-arm during mastication). Variables predicted to be related to ingestive behaviors were adjusted by dividing by mandibular length (as a measure of the load-arm during incision). Great ape genera were compared using a one-way analysis of variance (ANOVA) with a Tukey's honestly significant difference (HSD) test for multiple post-hoc comparisons. Data for each of the *Gorilla* and *Pongo* species were pooled because they differed in the same direction when compared to the other genera and differed in very few features of the TMJ (see Terhune, 2013). However, the data for *P. paniscus* and *P. troglodytes* were kept separate because of substantial differences between these two species. Results for similar analyses where all species were considered separately were virtually identical to those presented here. Males and females were pooled because there were no *a priori* expectations of functional differences between sexes, and because preliminary t-tests for significant differences in the univariate measurements suggested males and females do not differ in these measures of TMJ shape.

Geometric Morphometric Analyses

To standardize for differences in configurations related to orientation, size, and position, the 3D coordinates were first superimposed using Generalized Procrustes Analysis (GPA). To address the first research question, Procrustes distances among species and among genera were calculated to determine whether taxa were statistically distinct in morphospace, and the significance of each of these distances was assessed using a permutation test with 9,999 iterations. To correct for type I error, a sequential Bonferroni adjustment was employed (Rice, 1989). Variation in the sample was summarized and evaluated using principal components analysis (PCA), and shape variation along each axis was visualized using wireframe diagrams. Individual PC axes were regressed on the natural log of glenoid or condylar centroid size to examine whether shape variation along each axis varied allometrically. Each of these analyses (GPA, Procrustes distances, and PCA) was conducted separately for the glenoid and condylar configurations, and all taxa were included in these analyses. In all analyses, subspecies of *P. troglodytes* were pooled, as were males and females of each species, since there are no *a priori* expectations of functional differences among these groups. Landmark data were analyzed using the software programs *Morphologika* (O'Higgins and Jones, 1998) and MorphoJ (Klingenberg, 2011). Landmarks used in the GM analyses and their corresponding wireframe diagrams are listed in Table 1 and illustrated in Figure 1.

One problem GM analyses encounter when trying to address functional questions is the lack of an appropriate scaling variable. What does it mean to examine glenoid fossa shape as it relates to size of the glenoid fossa? As discussed in the introduction, analyses of masticatory variation most commonly incorporate mandible length (as a representation of the load arm during incision) and/or the distance from the TMJ to M_1 (i.e., the load arm during mastication on the posterior

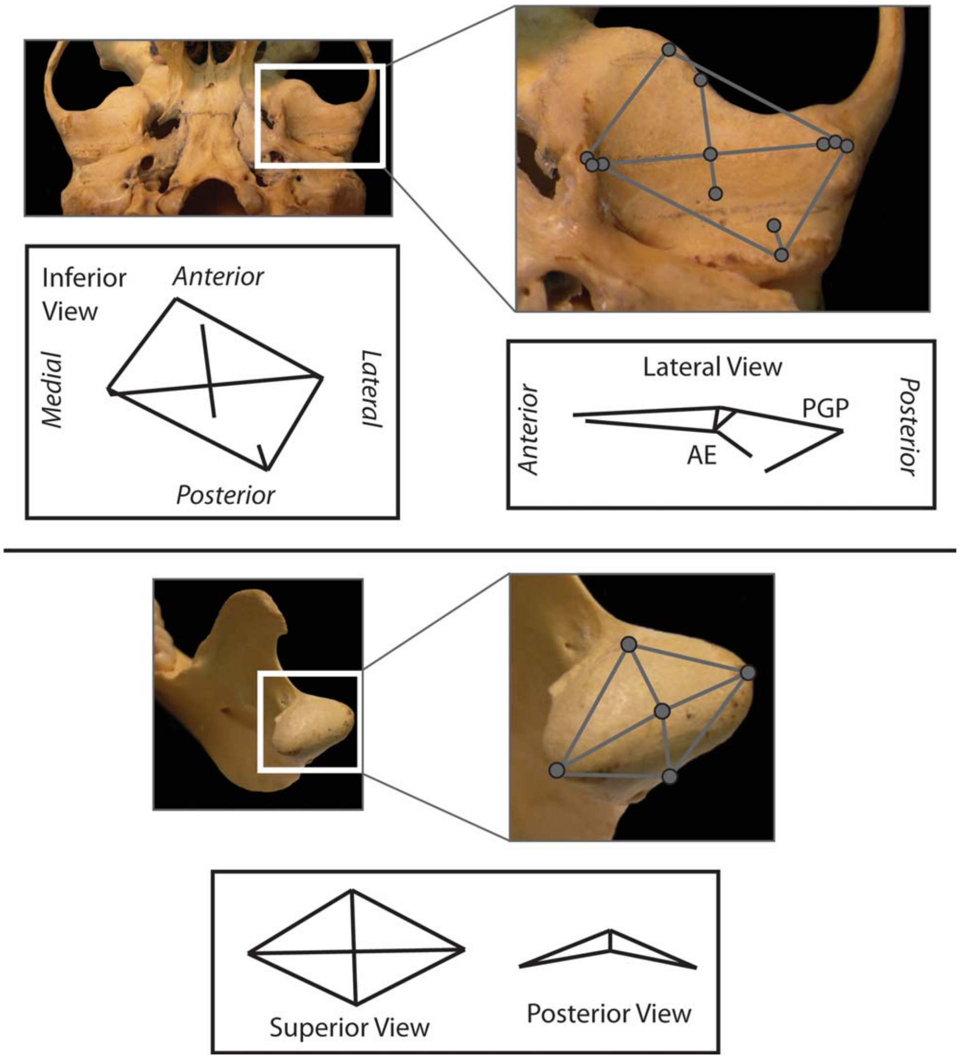

Fig. 1. *Pan troglodytes* glenoid (inferior view, top) and mandibular condylar (oblique view, bottom) showing landmarks and wireframe diagrams used in this study. Numbers correspond to landmarks listed in Table 1. Features indicated on the lateral view wireframe are the articular eminence (AE) and postglenoid process (PGP).

dentition). However, neither of these measures is encompassed by the coordinates of the glenoid fossa or mandibular condyle. To address this problem, I examine TMJ shape relative to the natural log of mandible length and relative to the natural log of the distance from the TMJ to M_1. Some researchers also suggest that scaling features relative to a geometric mean of multiple cranial dimensions is appropriate in analyses such as this (e.g., Jungers et al., 1995; Vinyard et al., 2003 [Appendix]; but see Vinyard, 2008); I therefore also examine TMJ shape variation relative to centroid size calculated from a configuration capturing the entire skull, which is analogous to a cranial geometric mean. Variation among taxa for each of these scaling variables was evaluated using one-way ANOVA with a Tukey's HSD test for multiple comparisons, and Pearson's product-moment correlations were calculated to assess covariation among these scaling variables.

TABLE 2. Comparative taxa used in this study

Species	Female	Male
Pan troglodytes schweinfurthii	12	12
Pan troglodytes troglodytes	7	9
Pan troglodytes verus	4	5
Pan paniscus	12	10
Gorilla beringei	8	10
Gorilla gorilla	12	12
Pongo abelii	9	10
Pongo pygmaeus	12	12

In this study I present two methods for incorporating biomechanical variables such as these into geometric morphometric analyses: multivariate regression (Monteiro, 1999) and a modification of Procrustes form space (Mitteroecker et al., 2004).

Regression analyses. First, I performed a multivariate regression and regressed the Procrustes coordinates of the configurations onto a biomechanically relevant variable. A permutation test with 9,999 iterations was performed to determine the significance of the regression, and shape variation along the regression line was examined using wireframe diagrams. Because all of the configurations had previously been scaled to unit centroid size, this analysis examines only allometric shape variation relative to the independent variable. In many ways this is analogous to regressing functional shape ratios, which have already been size-standardized, onto another size variable. Therefore, to more closely approximate functional scaling analyses (i.e., where the feature in question is regressed on a size variable in order to examine isometry or allometry), I further analyzed how form (i.e., size and shape) covaried with the biomechanical variables in question. For this analysis, size was added back to the Procrustes rotated coordinates by scaling the landmark coordinates by their original centroid size. By adding size back to the configurations in this way isometric shape variation is included in the analysis, as would be the case in traditional functional scaling analyses.

The multivariate regressions and permutation tests described above were performed for each independent variable. For both the regressions without size (shape regressions) and those that incorporated centroid size (form regressions), scaling relationships were analyzed for each species separately and for a pooled sample of all specimens. Again, the glenoid and condyle configurations were analyzed separately.

As in a traditional functional scaling analysis, these multivariate regressions identify whether the relationship between the dependent and independent variables is significant, and they also identify the percentage of the variance explained by the independent variable. However, these regressions do little to identify whether the shape or form trajectories differ across taxa. I therefore also examined the extent to which the regression trajectories for each of these species differed in morphospace by calculating an angle (i.e., the arccosine of the dot product) between the vectors of regression coefficients for each pair of species (e.g., McNulty et al., 2006). The significance of these angles was assessed using a permutation test with 9,999 iterations of the regression residuals (following Anderson and Ter Braak, 2003; Collyer and Adams, 2007; Adams and Collyer, 2009; Piras et al., 2010; Smith et al., in press). Because of the high number of statistical tests employed here, a sequential Bonferroni adjustment (Rice, 1989) was performed to guard against type 1 error. These analyses were performed in the program *R* (*R* Development Core Team, 2008) using the package *geomorph* (Adams and Otárola-Castillo, 2012).

Functional PCAs. The second method I present draws on size-shape space (i.e., Procrustes form space) as outlined by Mitteroecker et al. (2004). This method places size, which is represented as the natural log of the centroid size of the configurations being examined, back into the principal component analysis by including log centroid size as an additional variable in the calculation of the variance/covariance (V/CV) matrix. Because centroid size tends to have a higher variance than the Procrustes coordinates, including this variable in the V/CV matrix forces almost all of the size-related shape variation that is common to the entire sample onto the first axis of the subsequent principal components analysis. Compressing the size-related shape variation common to all specimens onto a single axis in this way is particularly useful in analyses that examine both multiple species and specimens across a wide range of sizes. This contrasts with PC 1 of a standard PCA for such a sample, that would instead represent a combination of size-correlated shape differences and shape differences among taxa not related to size (i.e., phylogenetic differences).

Although analyzing specimens in Procrustes form space does not add additional shape information to the analysis, the inclusion of a size variable in the V/CV matrix does augment the interpretation of shape space and the relationships among specimens in the subsequent PCA. For example, if one calculates Euclidean distances among specimens in a standard PCA, the distance between two specimens of similar shapes but different sizes would be relatively small. However, in form space the Euclidean distance among these same specimens is relatively large, simply because size has been used to augment the position of these specimens relative to one another. In fact, in the sample of glenoid configurations examined here, Euclidean distances between specimens in shape space show a low, although significant (r=0.211, $P < 0.001$), correlation with absolute differences among specimens in centroid size. In contrast, in form space Euclidean distances among specimens are highly significantly correlated with absolute centroid size ($r = 0.969$, $P < 0.001$).

Although incorporating the centroid size of the configuration being examined is appropriate in Procrustes form space analyses that are explicitly interested in the relationship between shape and centroid size, examining shape in relation to centroid size of the glenoid fossa or condyle is less likely to be meaningful from a biomechanical standpoint. Instead, I include a biomechanically relevant variable in the V/CV matrix that then compresses the variation related to this variable that is common to all taxa onto PC 1. Separate PCAs were performed using the natural log of each of the biomechanical scaling variables (i.e., mandible length, TMJ-M_1 distance, and skull centroid size). These V/CV matrices and PCAs were performed in SAS version 9.3 (SAS Institute, Inc., 2011) and their corresponding wireframes visualized using *Morphologika* (O'Higgins and Jones, 1998). These augmented PC analyses are referred to here as "functional PCAs."

RESULTS

Univariate Analyses

Glenoid fossa dimensions. Great ape taxa differ primarily in the relative anteroposterior (AP) dimensions of the glenoid fossa (Fig. 2). Preglenoid plane length (both relative to mandible length and AP length of the glenoid fossa) differs strongly among taxa. *Gorilla* has the AP shortest preglenoid plane, whereas *Pan* (both *P. paniscus* and *P. troglodytes*) have relatively AP longer preglenoid planes. However, overall glenoid length (as a proportion of mandible length and as a ratio of glenoid length to condyle length) is relatively large in *Gorilla* and

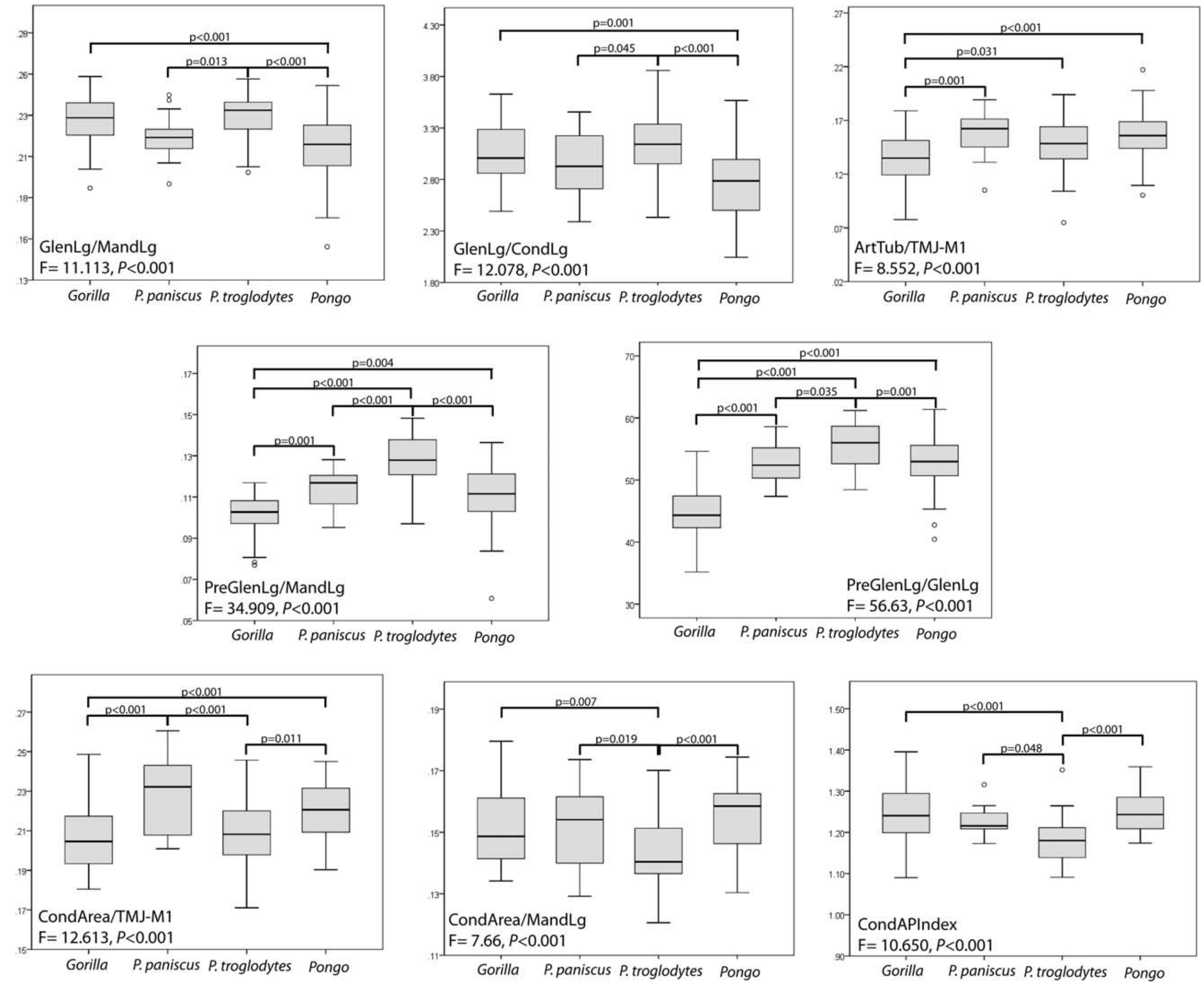

Fig. 2. Boxplots of univariate analyses (adapted from Terhune, 2013) their corresponding ANOVA results with the post-hoc *P*-values for multiple comparisons. Darkened bars represent the median value for each group, the boxes show the interquartile range (25th to 75th percentile), and the whiskers extend to 1.5 times the interquartile range. There were no statistically significant differences among taxa in relative condylar width (CondWid/TMJ-M_1: $F = 7.66$, $P = 0.311$), relative condylar length (CondLg/MandLg: $F = 2.025$, $P = 0.113$), or relative entoglenoid process projection (EntGl/TMJ-M_1: $F = 1.041$, $P = 0.376$).

P. troglodytes when compared to *Pongo*. Thus, gorillas tend to have a long glenoid but small preglenoid plane, which may indicate relatively less condylar translation in this clade compared to *Pan* and *Pongo* (Wall, 1999; Vinyard et al., 2003). Although there are no significant differences in relative entoglenoid process projection, articular tubercle projection (relative to TMJ-M_1 distance) is smallest in *Gorilla* when compared to all other taxa. The biomechanical significance of these two features is unclear, but experimental data suggest that the entoglenoid may act to guide movements of the mandibular condyle (Wall, 1995, 1999), while the articular tubercle (as the attachment for the temporomandibular ligament) likely acts to resist tensile forces at the joint (Greaves, 1978; Hylander, 1979; Spencer, 1995; Wall, 1995).

Condylar dimensions. *Pan* tends to have the relatively flattest condyle, while the mandibular condyle is relatively more curved in *Gorilla* and *Pongo*. This increased condylar curvature in *Gorilla* and *Pongo* may indicate increased condylar rotation in these taxa relative to *Pan*. Taxa also differ significantly in condylar area, which likely reflects differences in joint reaction forces. However, although the pattern of shape differences is roughly similar when condylar area is scaled relative to TMJ-M_1 distance and mandible length, more significant differences among taxa are apparent when condylar area is assessed relative to TMJ-M_1 distance. Relative to TMJ-M_1 distance, condylar area is smallest in *Gorilla* when compared to *Pongo* and *P. paniscus* (but not *P. troglodytes*), and is relatively larger in *Pongo* than *P. troglodytes*. However, when scaled by mandible length, condylar area is relatively larger in *Gorilla*, *Pongo*, and *P. paniscus* when compared to *P. troglodytes*, but there are no significant differences in condylar area among *Gorilla*, *P. paniscus*, and *Pongo*.

TABLE 3. Procrustes distances and corresponding *P*-values among species for the glenoid fossa (upper triangle) and mandibular condyle (lower triangle). All distances are statistically significant after sequential Bonferroni correction

	P. troglodytes	*P. paniscus*	*P. abelii*	*P. pygmaeus*	*G. beringei*	*G. gorilla*
P. troglodytes		0.0834 $P < 0.0001$	0.1118 $P < 0.0001$	0.0902 $P < 0.0001$	0.1819 $P < 0.0001$	0.1369 $P < 0.0001$
P. paniscus	0.0771 $P < 0.0001$		0.0865 $P < 0.0001$	0.1055 $P < 0.0001$	0.1502 $P < 0.0001$	0.0983 $P < 0.0001$
P. abelii	0.0453 $P = 0.016$	0.0595 $P = 0.013$		0.0799 $P = 0.0006$	0.1221 $P < 0.0001$	0.0959 $P < 0.0001$
P. pygmaeus	0.0888 $P < 0.0001$	0.0752 $P = 0.001$	0.061 $P = 0.02$		0.138 $P < 0.0001$	0.1325 $P < 0.0001$
G. beringei	0.0934 $P < 0.0001$	0.154 $P < 0.0001$	0.1219 $P < 0.0001$	0.1739 $P < 0.0001$		0.097 $P < 0.0001$
G. gorilla	0.0716 $P < 0.0001$	0.1058 $P < 0.0001$	0.0877 $P = 0.0007$	0.1435 $P < 0.0001$	0.0744 $P = 0.005$	

TABLE 4. Procrustes distances and corresponding *P*-values among genera for the glenoid fossa (upper triangle) and mandibular condyle (lower triangle). All distances are statistically significant

	Pan	*Pongo*	*Gorilla*
Pan		0.0827 $P < 0.0001$	0.1326 $P < 0.0001$
Pongo	0.0535 $P = 0.0001$		0.107 $P < 0.0001$
Gorilla	0.0837 $P < 0.0001$	0.1263 $P < 0.0001$	

Geometric Morphometric Analyses

Procrustes distances. The permutation test of Procrustes distances among group centroids found statistically significant distances among all pairs of taxa in shape space for both the glenoid fossa and mandibular condyle, even among congeners (Table 3). These distances were also statistically significant when species were lumped into genera (Table 4).

Principal components analysis. When variation in glenoid shape in the entire sample is examined (Fig. 3), *Gorilla* and *Pan* are relatively well differentiated along PC 1, but *Pongo* overlaps both groups considerably on this axis (which explains 29.2% of sample variance). There are also no strong patterns of shape variation between species within genera. Shape variation along PC 1 is associated with mediolateral (ML) and AP dimensions of the glenoid, as well as general relief of the joint. At the negative end of this axis *Pan* has a relatively AP long glenoid that is very flat, while at the positive end of the axis *Gorilla* has a very AP compressed glenoid that is ML wide and has considerably more topographic relief. This axis is also significantly related to glenoid centroid size ($r^2 = 0.3$, $P < 0.0001$). In contrast, PC 2 (17% of variation) does not consistently separate any of the taxa examined, and shape variation along this axis is relatively subtle (related primarily to entoglenoid and articular tubercle size and to the position of the most anterior point on the glenoid articular surface).

Principal component analyses of the condylar landmarks were less able to distinguish consistently among taxa. When all taxa were examined (Fig. 3), *Gorilla* and *Pongo* are roughly separated along PC 1 (although with considerable overlap), with the distribution for *Pan* overlapping both of these taxa entirely. This axis (48% of sample variance) was significantly related to condylar centroid size ($r^2 = 0.111$, $P < 0.0001$). Shape variation along this axis primarily reflects differences in AP length of the condyle (especially the posterior aspect of the articular surface), and ML convexity of the condyle. *Gorilla* loaded most positively on PC 1, and tends to have the most AP compressed and ML convex condyle. In contrast, *Pongo* and *Pan* tend to loaded more negatively and appear to have more AP elongated and ML flat condylar articular surfaces.

Biomechanical size variables. Correlations among the log-transformed size variables (mandible length, TMJ-M_1 distance, skull centroid size, glenoid centroid size, and condyle centroid size) indicate that all of these values are strongly correlated within each species (Table 5). The only correlation that was not statistically significant was for the natural log of mandible length (LnMandLg) versus glenoid centroid size in *P. paniscus*. When differences in mandible length, TMJ-M_1 distance, glenoid centroid size, and condyle centroid size are examined relative to skull centroid size, it is clear that taxa differ in these relative size measures as well (Fig. 4). *P. paniscus* and (to a lesser extent) *P. troglodytes* tend to have relatively smaller values when compared with *Pongo* and *Gorilla*. These data suggest that *Pan*, and particularly *P. paniscus*, appears to differ in these variables most consistently from the other taxa in this sample.

Shape regression analyses. The multivariate regressions of the fully GPA'd coordinates (e.g., shape) on the size variables (glenoid centroid size, mandible length, TMJ-M_1 length, and skull centroid size) indicate that when the entire sample is examined only about 10% of shape variation in the glenoid covaries with size, and ~6% of condylar shape variation was related to size (Table 6). However, although the relationship between the Procrustes residuals and each size variable is statistically significant at $P < 0.0001$ for the entire sample, these regressions largely fail to be significant at the species level, regardless of independent variable. The low percentage of variance explained by these regressions is

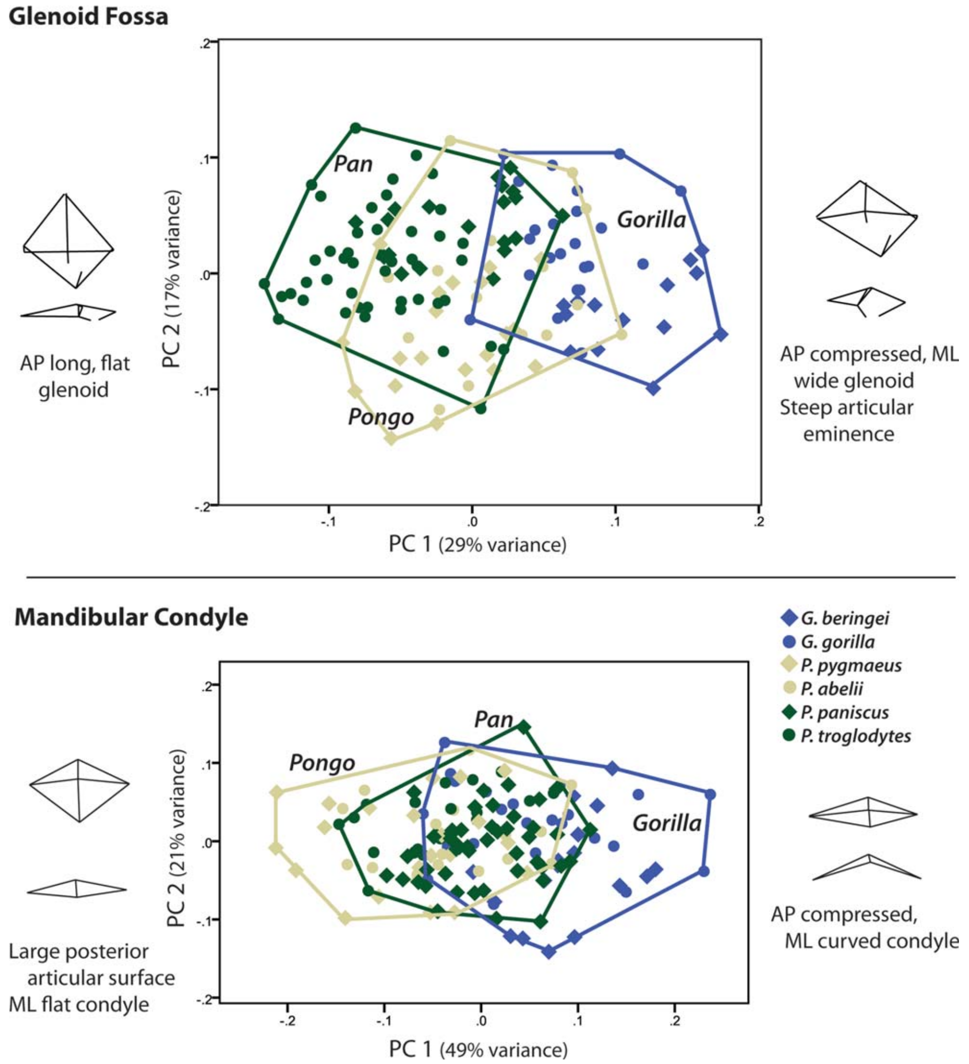

Fig. 3. Bivariate plots of the first two principal component (PC) axes for the glenoid (top) and mandibular condyle (bottom). Refer to Fig. 1 for interpretation of the wireframe diagrams.

likely explained by the initial scaling of each of these specimens to unit centroid size. As centroid size and each of the biomechanical scaling variables are strongly correlated, much of the size-related shape variation has been previously controlled for and isometric shape variation has been removed; the remaining variance explained is therefore that component of allometric shape variation that is related specifically to the biomechanical variables.

Visualization of the regression plots indicates that the pattern of shape variation differed only slightly depending upon the size variable examined, since all of these size variables covary strongly with one another. I therefore only present figures and discuss results for the shape coordinates regressed against LnMandLg here (Fig. 5). For the glenoid fossa configuration, this regression entirely separates the distributions for *Pan* and *Gorilla*, whereas *Pongo* is still largely intermediate. The distributions for *P. paniscus* and *P. troglodytes* are also entirely separate primarily due to the large difference in mandible length among these taxa. Shape variation along the regression vector is similar to the shape variation observed in the original PC plots, with bonobos and chimps having AP long, flat glenoids, whereas gorillas have AP shorter, ML wider glenoids with more topographic relief (Fig. 6). Angles between the regression trajectories indicate that the trajectories for *P. pygmaeus* and *P. paniscus* are the most distinct (Table 7, upper triangle).

As with the glenoid fossa, regression of the condylar coordinates on LnMandLg does a better job of differentiating among taxa than the standard PCA; again, the distributions for *Pan* and *Gorilla* are entirely separate, while *Pongo* is intermediate. Shape variation along the condylar regression vector reflects AP length and ML curvature of the condyle (Fig. 6). Angles between the regression trajectories indicate that the trajectories for *P. pygmaeus*, *P. troglodytes*, and *P. abelii* are the most distinct (Table 7, lower triangle).

Form regression analyses. The regression analyses of the GPA'd coordinates scaled by centroid size

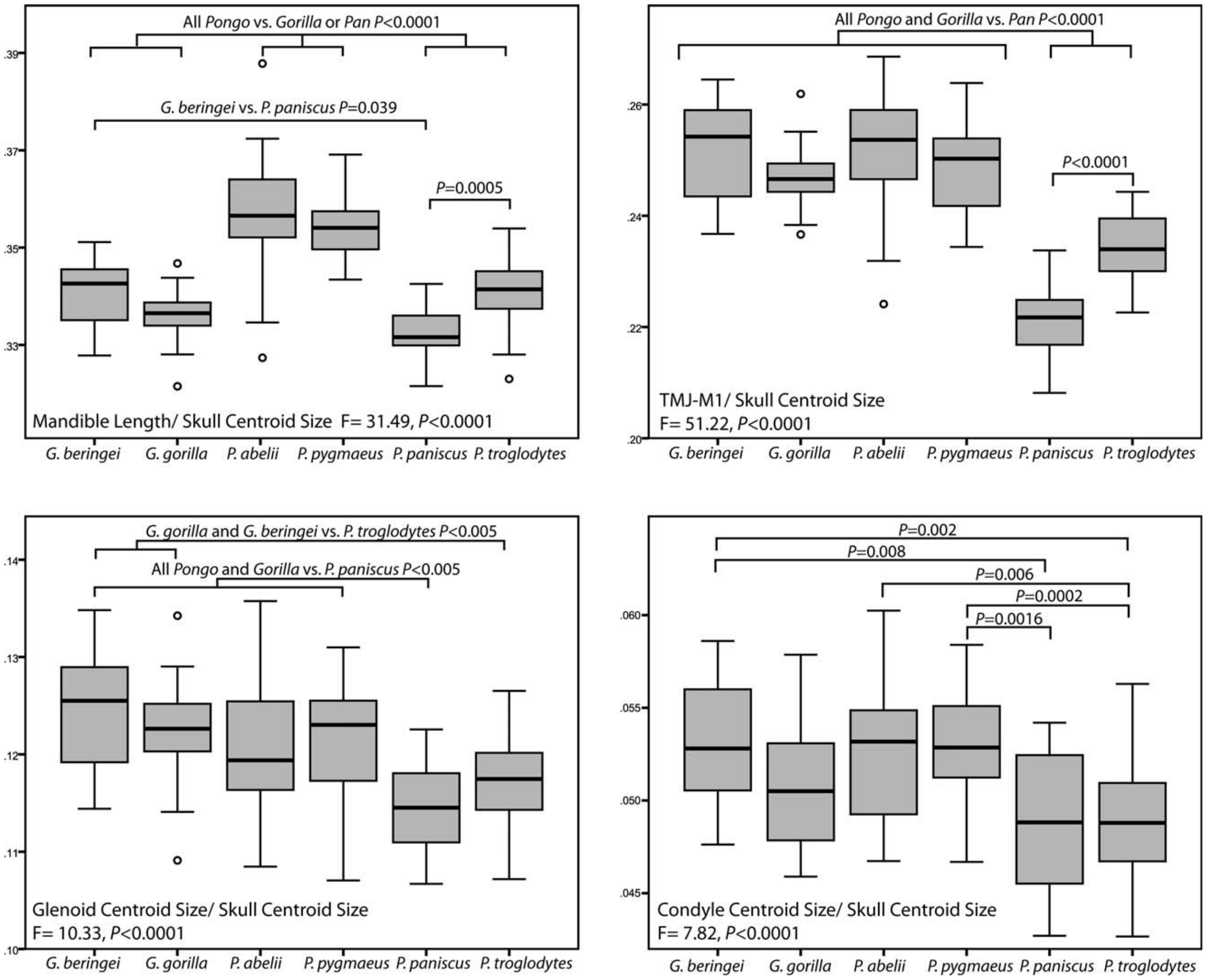

Fig. 4. Box plots of size variables scaled by skull centroid size and their corresponding ANOVA results with the post-hoc *P*-values for multiple comparisons. Darkened bars represent the median value for each group, the boxes show the interquartile range (25th to 75th percentile), and the whiskers extend to 1.5 times the interquartile range.

TABLE 5. Pearson product-moment correlation results for size variables

	G. beringei		*G. gorilla*		*P. abelii*		*P. pygmaeus*		*P. paniscus*		*P. troglodytes*	
Variables[a]	r	*P*-value	r	*P*-value	r	*P*-value	r	*P*-value	r	*P*-value	r	*P*-value
LnSkullCS vs.LnMandLg	0.98	<0.0001	0.65	0.0007	0.93	<0.0001	0.99	<0.0001	0.88	<0.0001	0.92	<0.0001
LnSkullCS vs. LnTMJ-M_1	0.94	<0.0001	0.98	<0.0001	0.92	<0.0001	0.98	<0.0001	0.83	0.0001	0.91	<0.0001
LnSkull CS vs. LnGlenCS	0.88	<0.0001	0.89	<0.0001	0.88	<0.0001	0.97	<0.0001	0.46	0.039	0.76	<0.0001
LnSkullCS vs. LnCondCS	0.79	0.0007	0.86	<0.0001	0.81	0.0001	0.90	<0.0001	0.58	0.007	0.51	0.0003
LnMandLg vs. LnTMJ-M_1	0.98	<0.0001	0.61	0.002	0.97	<0.0001	0.98	<0.0001	0.90	<0.0001	0.90	<0.0001
LnMandLg vs. LnGlenCS	0.84	0.0002	0.58	0.003	0.80	0.0004	0.95	<0.0001	0.42	0.064*	0.69	<0.0001
LnMandLg vs. LnCondCS	0.71	0.0014	0.55	0.007	0.65	0.002	0.92	<0.0001	0.49	0.029	0.49	0.0005
LnTMJ-M1 vs. LnGlenCS	0.80	0.0005	0.88	<0.0001	0.84	0.0001	0.94	<0.0001	0.46	0.042	0.74	<0.0001
LnTMJ-M1 vs. LnCondCS	0.65	0.0051	0.85	<0.0001	0.74	0.0003	0.91	<0.0001	0.54	0.013	0.51	0.0003
LnGlenCS vs. LnCondCS	0.82	0.0003	0.94	<0.0001	0.87	0.0000	0.92	<0.0001	0.66	0.001	0.72	<0.0001

All comparisons are statistically significant after sequential Bonferroni correction except for LnMandLg vs. LnGlenCS for *P. paniscus* (indicated with *)

[a] LnSkullCS = natural log of skull centroid size; LnMandLg= natural log of mandible length; LnTMJ-M_1= natural log of the distance from the mandibular condyle to M_1; LnGlenCS= natural log of glenoid centroid size; LnCondCS= natural log of condyle centroid size.

TABLE 6. Results of the shape and form regressions for each of the size variables

		Shape regressions				Form regressions			
		Glenoid Fossa		Mandibular Condyle		Glenoid Fossa		Mandibular Condyle	
Variables	N (glen/ cond)	%var	*P*-value	%var	*P*-value	%var	*P*-value	%var	*P*-value
Ln Configuration Centroid Size	138/148	**11.13**	**<0.0001***	**5.78**	**<0.0001***	**71.76**	**<0.0001***	**74.54**	**<0.0001***
G. beringei	14/17	4.57	0.847	7.97	0.262	**45.79**	**<0.0001***	**53.22**	**<0.0001***
G. gorilla	23/23	**12.63**	**0.003***	**12.46**	**0.041**	**51.07**	**<0.0001***	**55.25**	**<0.0001***
P. abelii	15/19	8.30	0.323	10.94	0.098	**53.02**	**<0.0001***	**57.60**	**<0.0001***
P. pygmaeus	20/22	6.38	0.273	**21.21**	**0.001***	**61.81**	**<0.0001***	**70.91**	**<0.0001***
P. paniscus	20/20	4.75	0.501	12.51	0.055	**18.86**	**0.0002***	**56.22**	**<0.0001***
P. troglodytes	46/47	3.66	0.088	4.45	0.066	**25.26**	**<0.0001***	**47.65**	**<0.0001***
Ln Mandible Length	138/148	**9.51**	**<0.0001***	**6.12**	**<0.0001***	**65.61**	**<0.0001***	**62.98**	**<0.0001***
G. beringei	14/17	10.83	0.158	9.59	0.180	**36.48**	**<0.0001***	**29.12**	**0.002***
G. gorilla	23/23	7.36	0.094	6.01	0.241	**38.05**	**<0.0001***	**17.15**	**0.012***
P. abelii	15/19	9.44	0.223	**15.37**	**0.030**	36.88	**0.0003***	**31.04**	**0.001***
P. pygmaeus	20/22	6.52	0.259	**23.19**	**0.001***	56.63	**<0.0001***	**61.81**	**<0.0001***
P. paniscus	20/20	3.79	0.709	7.26	0.212	5.76	0.3429	**15.42**	**0.033***
P. troglodytes	46/47	1.92	0.559	1.72	0.552	12.07	**<0.0001***	**12.25**	**0.001***
Ln TMJ-M$_1$	138/148	**10.14**	**<0.0001***	**6.09**	**<0.0001***	**66.46**	**<0.0001***	**65.25**	**<0.0001***
G. beringei	14/17	10.33	0.185	6.29	0.384	**33.11**	**0.0003***	**23.04**	**0.008***
G. gorilla	23/23	7.05	0.111	**14.12**	**0.027**	**38.57**	**<0.0001***	**42.92**	**<0.0001***
P. abelii	15/19	10.23	0.171	15.70	0.028	**40.00**	**<0.0001***	**37.08**	**<0.0001***
P. pygmaeus	20/22	5.98	0.324	**18.71**	**0.006***	**56.23**	**<0.0001***	**58.26**	**<0.0001***
P. paniscus	20/20	3.83	0.699	10.93	0.082	6.23	0.2823	**19.79**	**0.012***
P. troglodytes	46/47	2.35	0.375	1.34	0.681	**13.89**	**<0.0001***	**13.08**	**0.001***
Ln Skull Centroid Size	138/140	**10.86**	**<0.0001***	**6.29**	**<0.0001***	**68.68**	**<0.0001***	**66.65**	**<0.0001***
G. beringei	14/14	10.26	0.186	9.34	0.291	**38.85**	**<0.0001***	**36.03**	**0.002***
G. gorilla	23/23	7.43	0.081	14.44	0.023	**39.57**	**<0.0001***	**43.77**	**<0.0001***
P. abelii	15/17	8.35	0.306	14.77	0.058	**42.01**	**<0.0001***	**42.21**	**<0.0001***
P. pygmaeus	20/20	6.35	0.274	18.26	0.011	**58.62**	**<0.0001***	**53.45**	**<0.0001***
P. paniscus	20/20	5.69	0.350	5.81	0.324	8.13	0.1077	**19.83**	**0.011***
P. troglodytes	46/46	2.43	0.342	0.81	0.886	**14.83**	**<0.0001***	**11.64**	**0.001***

Data are presented both for the entire sample and for each species separately. Bolded values are significant at $P < 0.05$, starred *P*-values are significant after sequential Bonferroni correction. %var= percentage variance explained by the regression.

identified significant relationships between the Procrustes residuals and the size variables (mandible length, TMJ-M$_1$ length, and centroid size) for almost all analyses (Table 6). When the entire sample is examined, these regressions explain between 66 and 72% of the size and shape variation for the glenoid, and between 63 and 75% of size and shape variation is explained for the condyle. Regression analyses for each species are highly variable; for all size variables, the lowest amount of variation is explained for *P. paniscus*, and these relationships are not significant when glenoid form is regressed on mandible length, TMJ-M$_1$ distance, or skull centroid size. However, regression of mandibular condyle form identified statistically significant regression relationships for all taxa and all size variables.

Visualization of the regression plot of LnMandLg demonstrates a stronger relationship between size and form than was observed when the specimens were fully GPA'd (Fig. 5). Again, glenoid form in *Pan* and *Gorilla* is strongly differentiated, and *Pongo* lies intermediate between these two groups. Furthermore, the distribution for *P. paniscus* is entirely separate from all other taxa. Only the angle between the regression trajectories for *P. pygmaeus* and *P. abelii* was statistically significant after Bonferroni correction (Table 8). In the mandibular condyle, regression of the scaled Procrustes residuals on LnMandLg results in a stronger overlap between *Pongo* and *Gorilla*, but the distributions for *Gorilla* and *Pan* remain similarly differentiated. No angles between the regression trajectories for the condyle were statistically significant after Bonferroni correction (Table 8).

Principal components analysis incorporating biomechanical variables. Incorporating the biomechanically relevant scaling variables into the V/CV matrix of the principal components analysis considerably changes the visualization of specimens in morphospace for both the glenoid and the condyle (Fig. 7). As with the regression analyses, I present only results for the V/CV using mandible length, but results for all analyses were very similar because of the high degree of covariance among the biomechanical scaling variables.

When the glenoid fossa configuration is examined, PC 1 (which explains 67% of the shape variance) entirely separates the distributions for *Pan* and *Gorilla*, as well as *P. paniscus* and *P. troglodytes*. Again, *Pongo* is intermediate between *Gorilla* and *Pan*. *G. beringei* also loads more positively along PC 1 than does *G. gorilla*, although there is still considerable overlap between these two species. Unsurprisingly, this axis is strongly correlated with LnMandLg (r^2=0.994, $P < 0.0001$). On PC 2 (which explains 28% of the variance), all three genera overlap, though there is a substantial separation

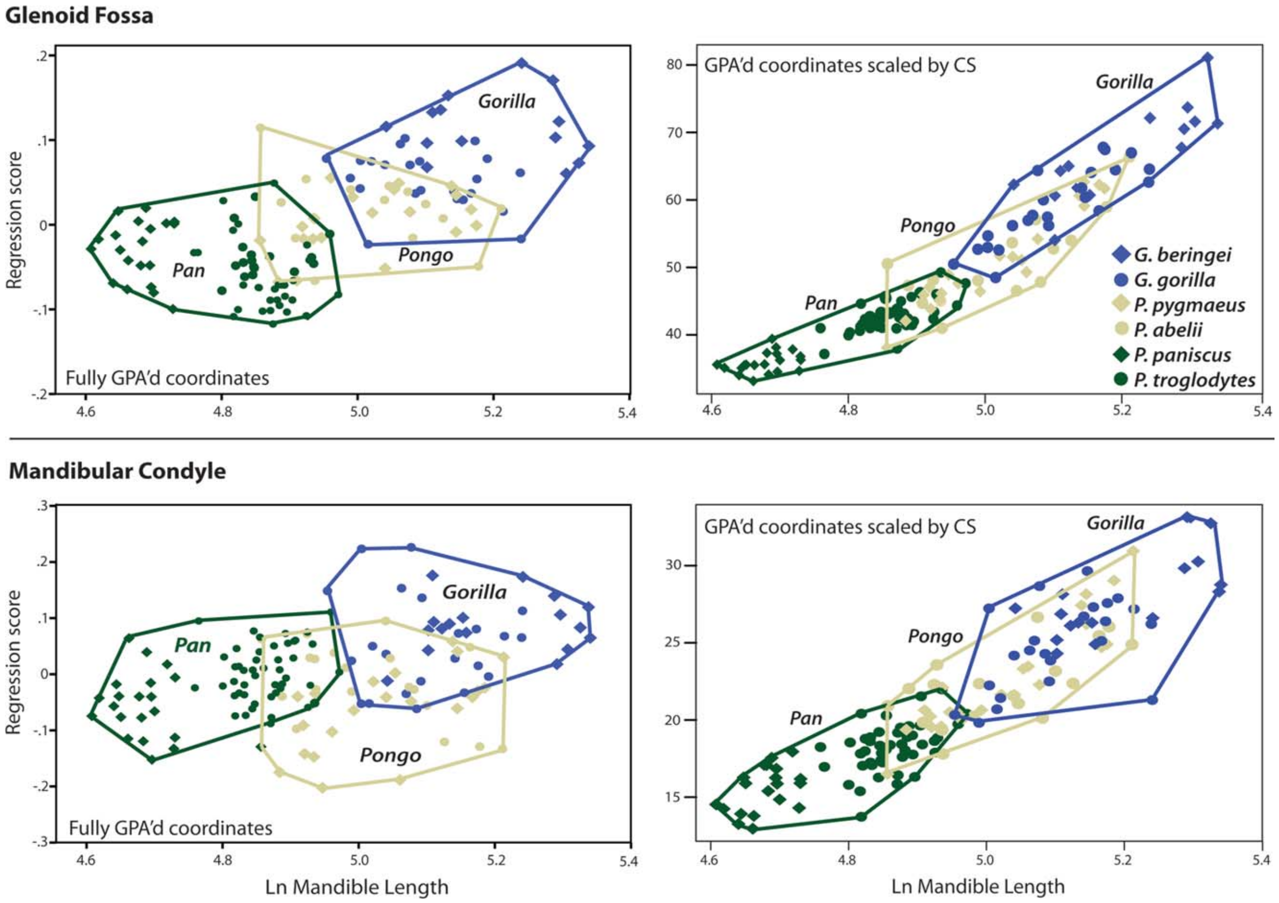

Fig. 5. Bivariate plots of the multivariate regression scores for the glenoid (top) and condyle (bottom) against the natural log of mandible length. Plots on the left of the figure show fully GPA'd coordinates (shape) regressed on the natural log of mandible length; plots on the right of the figure show the GPA'd coordinates scaled by size (form) regressed on the natural log of mandible length.

between *P. paniscus* (which loads more negatively) and *P. troglodytes* (which loads more positively). *Pongo* also tends to load more positively along this axis than *Gorilla*. Wireframe diagrams of shape variation along these two axes suggest that *Pan* and *Pongo* both tend to have relatively flatter, AP longer glenoids than does *Gorilla,* as does *P. troglodytes* when compared to *P. paniscus*.

For the condylar configuration, *Gorilla* and *Pan* are also strongly differentiated along PC 1 (which accounts for 71% of the sample variance). Again, this axis is highly correlated with LnMandLg ($r^2 = 0.994$, $P < 0.0001$). As in the standard PCA, PC 1 represents variation in the size of the posterior condylar articular surface and the ML curvature of the condyle. PC 2 also largely reflects this same shape variation; thus gorillas, which load positively on PC 1 and negatively on PC 2, tend to have flatter condyles that are AP compressed when compared to both Pongo and Pan.

DISCUSSION

The great apes are a diverse, well-studied group of primates that encompass a variety of feeding behaviors (e.g., Badrian and Malenky, 1984; Watts, 1984; Williamson et al., 1990; Tutin and Fernandez, 1993; Lucas et al., 1994; Elgart-Berry, 2004; Vogel et al., 2008). These factors make the great apes an ideal clade in which to assess the degree to which features of the TMJ are linked to these documented differences in feeding behavior, and to compare and contrast univariate and multivariate methods for assessing functional shape variation. Previous analyses of great ape masticatory morphology provide conflicting reports as to whether the shape of the masticatory apparatus accurately reflects these behavioral differences (Krogman, 1931a,b; Schultz, 1969; Daegling, 1989, 2007; Taylor, 2002, 2005, 2006a,b; Constantino, 2007; McCollum, 2007; Taylor et al., 2008). The data presented here and in Terhune (2013) are no exception.

Comparing the Univariate and Geometric Morphometric Analyses

Univariate analyses of great ape TMJ form (Terhune, 2013) suggest that much of the variation in the glenoid fossa and condyle of the great apes is linked to differences in AP dimensions of this joint. However, perhaps with the exception of the preglenoid plane—which shows strong differentiation among taxa—these differences are

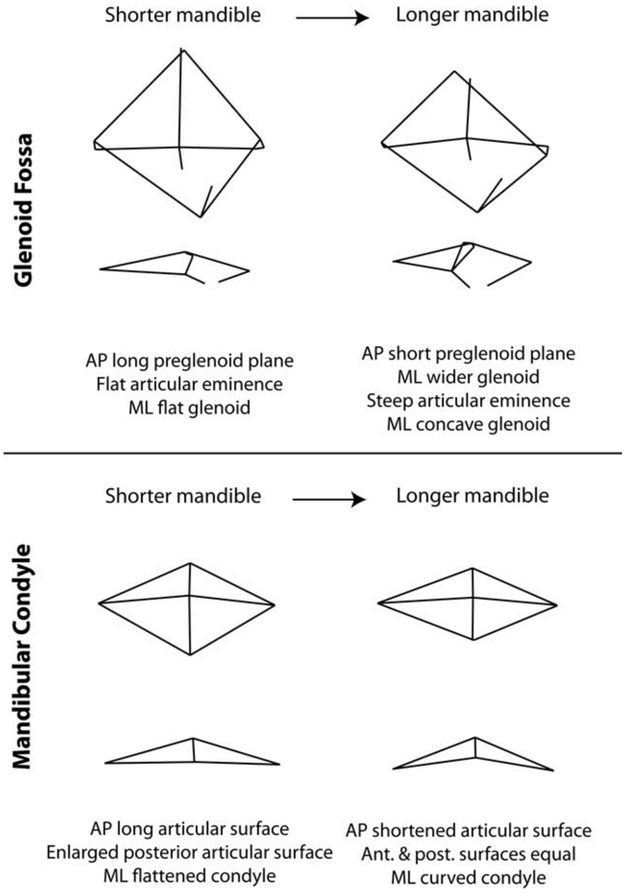

Fig. 6. Wireframe diagrams for the glenoid (top) and condyle (bottom) describing shape variation related to mandibular length. Refer to Fig. 1 for interpretation of the wireframe diagrams.

relatively subtle. Several features that were originally predicted to vary in relation to joint reaction forces (Terhune, 2013) failed to be significantly different among taxa, or did not vary in a systematic way. For example, the results for condylar area differ depending upon the scaling variable employed. This feature did not conform to my original predictions that condylar area would be relatively larger in *Gorilla* and *Pongo* compared to *Pan*, and this result may suggest that taxa do not differ strongly in their ability to dissipate reaction forces at the TMJ. Furthermore, these univariate data suggest that *Pongo* is largely intermediate in TMJ form between *Gorilla* and *Pan*, and that there are substantial differences in TMJ form between *P. paniscus* and *P. troglodytes*.

The results of the GM analyses are largely consistent with the univariate results but allow for a more nuanced examination of shape differences among taxa. Interestingly, the Procrustes distances among all taxa were significant, suggesting that there are substantial differences in TMJ shape among all species and genera that are not reflected in the univariate data. This result directly addresses my first research question, which asked whether taxa differ significantly in TMJ shape when analyzed using GM methods. However, the significant Procrustes distances were difficult to visualize using a standard PCA. Instead, taxa overlapped considerably on all of the top PC axes, which each explained relatively small amounts of the sample variance.

Incorporating a biomechanically relevant variable such as mandible length, either via regression or by inclusion in the V/CV did help to visually differentiate taxa further. Although these analyses do not change the initial relationships of the specimens in shape space, augmenting the visualizations in these ways helps to more easily identify shape variation that may be functionally significant. For example, in both the regression analysis and functional PCAs, *Gorilla* and *Pan* were strongly differentiated in the regression plots and along the top PC axes, whereas *Pongo* again appeared largely intermediate in form. Separation of taxa in these plots also extended below the generic level, with *P. paniscus* and *P. troglodytes* strongly separating from one another. *G. beringei* and *G. gorilla* were also differentiated from one another when assessed relative to a biomechanical variable, although this separation was less distinct. This differentiation appears to be largely due to the strong differences in absolute and relative mandible length among these taxa. Thus, shape variation along the regression vectors, or along PC 1 in the functional PCAs, reflects glenoid shape or form variation in relation to mandible length, an important measure of lever arm length during incision (Bouvier, 1986a,b; Hylander, 1985; Vinyard, 2008).

Masticatory Variation in the Great Apes

Given these data, what can we infer about great ape TMJ function? Previous research examining great ape masticatory shape has revealed some differences in condylar dimensions among taxa. Taylor (2002, 2005, 2006) found few ontogenetic or adult differences in condylar shape between *P. paniscus* and *P. troglodytes*, despite documented behavioral differences between these species. However, Taylor (2005) did identify wider mandibular condyles in mountain gorillas (*G. beringei*) relative to all other African apes, and she similarly identified that all gorillas showed this same feature relative to *Pan*. Taylor (2006) also found that Bornean orangutans have relatively larger condyles than Sumatran orangutans, a result which is consistent with observations that *P. pygmaeus* tends to rely on more resistant foods than does *P. abelii*. This prior work hints at differences in TMJ shape among taxa, but no direct comparisons of TMJ form among great ape genera have been previously conducted, and no studies have examined the cranial component of this functionally important joint.

Documented behavioral differences suggest a gradient in dietary resistance (e.g., fracture toughness and/or stiffness) among great ape genera, with members of *Pan* perhaps consuming the least resistant foods and *Pongo* consuming the most resistant foods (Elgart-Berry, 2004; Vogel et al., 2008). However, these data are limited to a single species in each genus, and they do not reflect the frequency at which exceptionally resistant or moderately resistant foods are consumed. For example, it is well known that *G. beringei* rely heavily on food items such as THV that require cyclical loading of the mandible to process (Elgart-Berry, 2004). In contrast, behavioral data suggest that orangutans utilize exceptionally resistant food items that require very high occlusal forces (e.g.,

TABLE 7. Angles (in degrees) between species trajectories for the glenoid (upper triangle) and condyle (lower triangle) when shape was regressed on the natural log of mandible length

	P. troglodytes	*P. paniscus*	*P. abelii*	*P. pygmaeus*	*G. beringei*	*G. gorilla*
P. troglodytes		75 $P = 0.54$	68 $P = 0.53$	**98** **$P < 0.0001$***	67 $P = 0.59$	78 $P = 0.29$
P. paniscus	**99** **$P < 0.0001$***		63 $P = 0.82$	**93** **$P < 0.0001$***	50 $P = 0.97$	**93** **$P < 0.0001$***
P. abelii	**109** **$P < 0.0001$***	72 $P = 0.40$		24.08 $P = 0.10$	69 $P = 0.46$	59 $P = 0.70$
P. pygmaeus	53 $P = 0.65$	77 $P = 0.29$	**45** **$P = 0.0013$***		**96** **$P < 0.0001$***	77 $P = 0.20$
G. beringei	86 $P = 0.07$	46 $P = 0.84$	**106** **$P < 0.0001$***	56 $P = 0.53$		83 $P = 0.13$
G. gorilla	83 $P = 0.13$	78 $P = 0.28$	63 $P = 0.45$	**98** **$P < 0.0001$***	71 $P = 0.32$	

Bolded values are significant at $P < 0.05$, starred *P*-values are significant after sequential Bonferroni correction. %var= percentage variance explained by the regression.

TABLE 8. Angles (in degrees) between species trajectories for the glenoid (upper triangle) and condyle (lower triangle) when form (shape and size) was regressed on the natural log of mandible length

	P. troglodytes	*P. paniscus*	*P. abelii*	*P. pygmaeus*	*G. beringei*	*G. gorilla*
P. troglodytes		36 $P = 0.51$	**40** **$P = 0.036$**	18 $P = 0.60$	26 $P = 0.31$	24 $P = 0.40$
P. paniscus	44 $P = 0.23$	$P = 0.51$	34 $P = 0.58$	30 $P = 0.77$	24 $P = 0.54$	33
P. abelii	24 $P = 0.32$	42 $P = 0.25$		**128** **$P < 0.0001$***	**47** $P =$ **0.002**	31 $P = 0.06$
P. pygmaeus	27 $P = 0.13$	48 $P = 0.12$	**88** **$P = 0.021$**		18 $P = 0.41$	**31** **$P = 0.05$**
G. beringei	27 $P = 0.23$	38 $P = 0.38$	28 $P = 0.05$	26 $P = 0.09$		28 $P = 0.13$
G. gorilla	28 $P = 0.16$	52 $P = 0.08$	21 $P = 0.33$	19 $P = 0.39$	31 $P =$ **0.02**	

Bolded values are significant at $P < 0.05$, starred *P*-values are significant after sequential Bonferroni correction. %var= percentage variance explained by the regression.

Vogel et al., 2008). These data set up a distinction between taxa that frequently experience only moderate masticatory stresses (as in *Gorilla*) vs. those that may infrequently experience extremely high stresses (as in *Pongo*). Although this is most certainly a simplified description of complex feeding behaviors, such a scenario outlines two extremes of the spectrum of masticatory behaviors, and it is unclear how we should expect the masticatory morphologies of taxa such as these to compare.

On the basis of the food material property data, previous authors have hypothesized that the masticatory apparatus of *Pongo* should be more robust than that of *Pan* or *Gorilla*, so that members of this genus can accommodate the increased masticatory loads associated with resistant foods. However, previous morphological work has failed to demonstrate that *Pongo* displays any features of the masticatory apparatus that can be linked to this increased dietary resistance (Daegling, 1989, 2007; Constantino, 2007), and bite force estimates are only highest in *Pongo* when maximum fracture toughness values of nonfruit, nonleaf vegetation were used to estimate bite force (Taylor et al., 2008). As with previous work, both the univariate and GM analyses presented here fail to support the assertion that the masticatory apparatus of *Pongo* is more robust than *Gorilla,* and instead place *Pongo* intermediate in TMJ form between *Gorilla* and *Pan*.

Similarly, although behavioral data indicate that *P. paniscus* tends to rely more consistently on terrestrial herbaceous vegetation (THV) than does *P. troglodytes*, previous analyses have found few morphological differences in the masticatory apparatus of these species (e.g., Taylor, 2002, 2005). Some researchers have suggested that this lack of morphological differentiation may be due to the fact that *P. paniscus* does not rely heavily on THV at all feeding sites (Chapman et al., 1994). However, the data presented here and in Terhune (2013) are consistent with improved load resistance in *P. paniscus* relative to *P. troglodytes*, as evidenced by the relatively larger condylar area, ML wider joints, and more inclined articular eminences observed in *P. paniscus*.

What is clear from both the univariate and multivariate data presented here, as well as from previous studies of great ape masticatory form (Daegling, 1989, 2007; Taylor, 2002, 2003, 2005, 2006; Constantino, 2007) is that there does not appear to be a straightforward relationship between food material property and/or

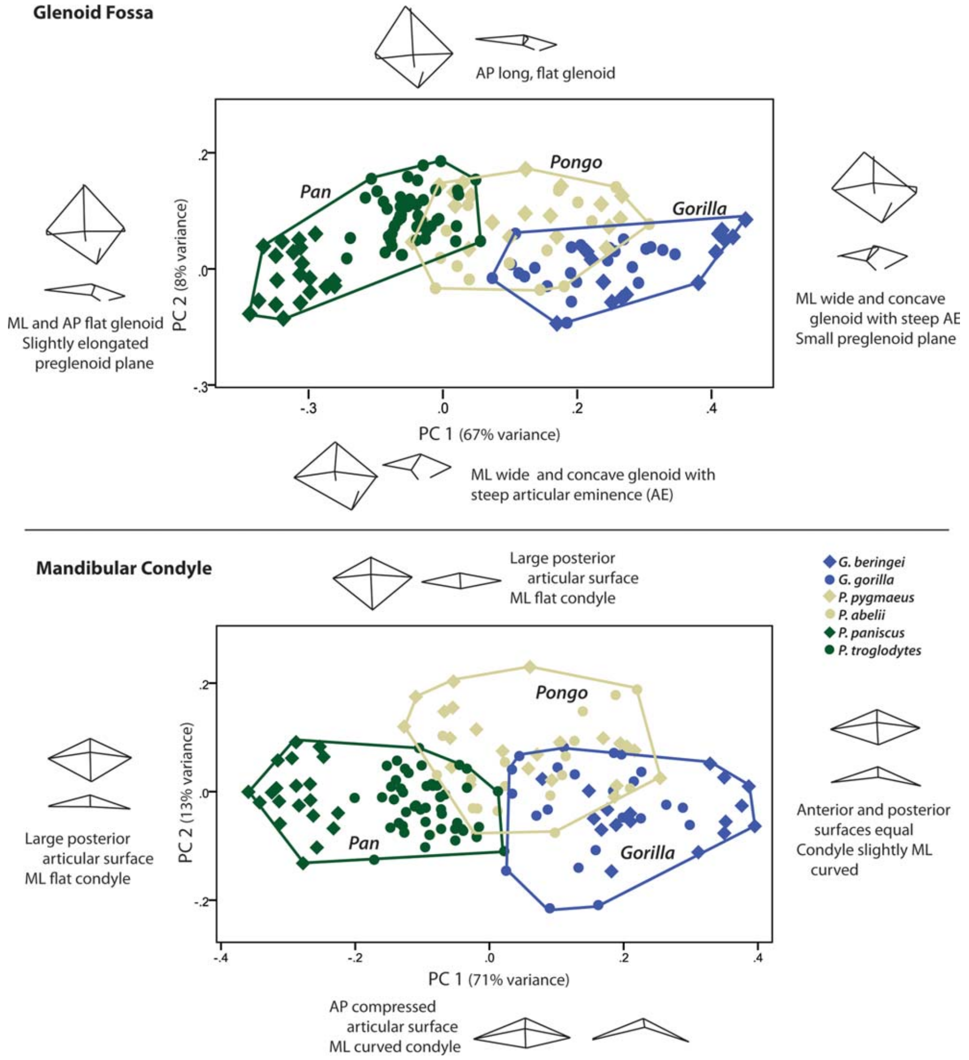

Fig. 7. Bivariate plots of the first two principal component (PC) axes for the glenoid (top) and mandibular condyle (bottom) from the functional PCAs where mandible length was included in the variance/covariance matrices. Refer to Fig. 1 for interpretation of the wireframe diagrams.

behavioral data and the ability of the masticatory apparatus to resist the loads generated to perform these feeding behaviors. One potential reason for this lack of a clear relationship is that perhaps other features in the joint are acting to mediate joint loads. The feature most clearly linked to load resistance in the TMJ is condylar area; increasing condylar area spreads joint loads out over a larger area of the glenoid fossa, decreasing stresses in the joint. Mediolaterally wide condyles have also been suggested to reflect high joint reaction forces in the lateral aspect of the TMJ, as would be produced by twisting of the mandibular corpus during the power stroke (Hylander, 1979, 2006; Hylander and Bays, 1979; Bouvier, 1986a). However, these features do not vary predictably among great ape taxa. Perhaps soft tissue structures are mediating these joint forces, or it is possible that articular eminence (AE) morphology influences joint loading (Terhune, 2011). Although it is not possible to evaluate the role of soft tissue structures here, *Gorilla* and *Pongo* do tend to have relatively more inclined AEs than does *Pan*. This feature may therefore represent a morphology for which there are few experimental data with which to formulate a prediction, but which is easily evaluated using GM methods.

Although these data suggest we are limited in our ability to infer the loading regimes of great ape taxa based on masticatory morphology, the overall form of the TMJ does vary strongly among these taxa and may instead be a better reflection of mandibular range of motion. As with the food material property data, ingestive behaviors have also been documented to vary among great ape taxa, with *Pongo* and *Pan* tending to rely more heavily on their anterior dentition for food processing (Ungar, 1994; Lambert, 1999). The strong differences in the anteroposterior dimensions of the glenoid fossa and mandibular condyle likely reflect differences in the amount of sagittal sliding (Wall, 1999) that occur at the TMJ in these taxa. Whether these apparent differences in range of motion are indicative of quantitative differences in maximum jaw gape requires further investigation.

Is the Observed Shape Variation Consistent Between Methods?

My second and third research questions asked whether the GM analyses observed the same shape variation as seen in the univariate data and whether the GM analyses were able to identify any additional features of the TMJ that varied among taxa. For the most part, these two methods identified the same patterns of shape variation among taxa. Both the univariate data and the GM analyses primarily suggest that shape differences among taxa are related to changes in the anteroposterior dimensions of the glenoid fossa and mandibular condyle. However the GM analyses demonstrated morphological differences among taxa linked to differences in the overall topography of the glenoid fossa that were not obvious in the univariate data (e.g., relative entoglenoid process size). Several features that were not examined in the univariate analyses were also observed to vary among taxa, including articular eminence (AE) inclination and mediolateral condylar curvature. Although relative condylar area was examined in the univariate study, the univariate analysis was unable to reveal the striking differences observed in the size of the posterior condylar articular surface, which is enlarged in *Pan* and *Pongo*. These results therefore suggest that there are indeed aspects of TMJ shape variation among taxa not revealed by the univariate data.

The Importance of Biomechanical Variables in GM Analyses

As evidenced by the Procrustes distances, species and genera differ significantly in shape space even before a biomechanical variable is incorporated into the analysis. However, this separation in morphospace is not clear using a standard PCA, and it was not until a biomechanically significant variable was incorporated into the GM analyses that any of the taxa were differentiated visually. These results suggest that assessing shape variation in relation to a biomechanically significant variable augments the existing shape variation in such a way that visualization and interpretation of the existing shape variation is facilitated. The results for *P. troglodytes* and *P. paniscus* provide a case in point. *P. paniscus* has a significantly shorter mandible relative to overall skull size than does *P. troglodytes*; biomechanically, shorter mandibles result in shorter lever arms during biting on the anterior dentition. Changes in lever arm length relative to the load arm have important implications for masticatory function; assuming that muscle forces are held constant, smaller lever to load arm ratios allow more of the muscle force to be converted into bite force, thereby increasing bite force while decreasing joint reaction force. However, although *P. paniscus* may have more efficient leverage than *P. troglodytes*, the results here suggest that *P. paniscus* displays several features linked to increased joint loading (e.g., larger mandibular condyles, ML wider joints, and a more inclined articular eminence [Bouvier, 1986a,b; Terhune, 2011). This may indicate that *P. paniscus* is capable of recruiting relatively larger muscle forces that in turn result in increased bite forces and increased joint reaction forces when compared to *P. troglodytes,* or could suggest that the TMJ of *P. paniscus* is overdesigned. Importantly, the glenoid morphology of *P. paniscus* is markedly different from that of *P. troglodytes*, the TMJ of which appears to be optimized for increased range of motion rather than load resistance. Some of these differences were apparent in the univariate data. However, the standard PCA failed to consistently differentiate among these taxa. By incorporating a biomechanical variable, the GM analyses were better able to differentiate between *P. paniscus* and *P. troglodytes*, and therefore were better able to replicate the univariate results.

Although I focus on the utility of mandible length as a biomechanical variable against which to assess shape variation, the pattern of shape variation relative to glenoid centroid size, skull centroid size, and the distance from the TMJ to M_1 was very similar as all of these variables are highly correlated. However, although centroid size and mandibular length covary here and yield very similar results, in taxa where centroid size and mandible length show a markedly different scaling relationship (e.g., Old World monkeys), taxa may show a fundamentally different pattern of shape variation. Additionally, other biomechanically important variables may prove useful for evaluating the functional significance of shape variation. In the masticatory apparatus, such variables may include the height of the TMJ above the occlusal plane, or perhaps lever to load arm ratios; similar analyses examining the postcranium could include body mass, a geometric mean of the region under investigation, or other relevant lever arm measures.

Methodological Strengths and Weaknesses

Univariate analyses of shape variation have a long history of use in physical anthropology and are by no means inappropriate for testing functional hypotheses. Yet these analyses only have the power to identify differences in shape variation in features that are explicitly assessed. Similarly, there is little doubt that geometric morphometric methods are useful for exploring and analyzing complex shape variation. However, the utility of this tool for examining functional morphology is debated (Baab et al., 2012). The data presented here indicate that GM can be a powerful tool for assessing functionally significant shape variation, and incorporating biomechanically significant variables in either of the ways proposed here is a simple method for placing these complex shape data into a biomechanical framework similar to that of univariate shape analyses.

Caution is of course warranted in the implementation of GM methods in functional analyses, since care should be taken to incorporate only those features that are functionally relevant. The results of this study are perhaps a bit of a red herring in that if the univariate analyses had evaluated other features (e.g., ML condylar curvature or posterior condylar articular surface area), the results of these two methods may have been more comparable. However, one major limitation of univariate analyses such as the one presented here is that they are restricted to those features that have a specific foundation in the existing biomechanical literature, which is why these (and other) features were not examined. It goes without saying that foundational experimental and theoretical work will continue to be necessary for evaluating functional shape variation; this is an area in which geometric morphometrics currently has little insight (but see O'Higgins et al., 2011).

One conclusion of this study should not be that morphologies examined using GM methods should not have a strong biomechanical framework; instead, GM methods are more amenable to the inclusion of features for which the functional significance is unclear. One way in which we may be able to maximize the utility of these methods for examining functional differences among taxa is to alter the way in which we phrase our biomechanical hypotheses. For example, while many biomechanical predictions highlight specific features that are expected to vary in a particular direction, perhaps GM analyses would best be served by more holistically addressing how the shape of the entire region may or may not vary in relation to function. An additional difficulty with testing specific hypotheses using GM methods is that, unlike traditional methods, *P*-values are likely to be linked to overall differences in shape (e.g., Procrustes distances among specimens or taxa). In the skull, for example, space is at a premium; cranial morphology is therefore a result of complex interactions between multiple functional, developmental, and phylogenetic demands. For instance, the glenoid fossa, although most tightly linked to masticatory function, may also vary in relation to functional units immediately surrounding the joint (e.g., hearing, balance, posture). Morphometric analyses designed to assess functional variation should therefore be coupled with further analyses that assess shape variation in a larger functional and morphological context. One way in which we might be able to at least partly limit our analyses to functionally relevant morphologies is to extract only those components of shape variation (e.g., PC axes or regression scores) that are significantly correlated with a biomechanical variable. These data, which should more closely reflection function, could then be the subject of further analysis. Finally, phylogenetic inertia and/or constraint likely play an important role in governing shape variation. Although the limited taxonomic scope of this study does not necessitate an extensive consideration of phylogeny, taxonomically broader analyses should employ appropriate phylogenetic controls and/or analyses designed to assess the presence or absence of a phylogenetic signal (e.g., Felsentein, 1985; Nunn and Barton, 2001; Klingenberg and Gidaszewski, 2010; Nunn, 2011).

There is no reason that the best of both of the methods contrasted here cannot be employed profitably to better understand functional shape variation. As demonstrated in this study, some baseline understanding of variation in the biomechanical variables of interest is necessary, and this assessment is most easily employed in a univariate context. Simple evaluations of relative differences in these variables are powerful tools for further examining how and why multivariate shape differences might vary among taxa. The first step in any GM analysis that incorporates a biomechanical variable that is external to the landmark configuration in question should be a univariate analysis of the biomechanical variables themselves. Furthermore, if specific morphological features are of interest as a result of either previous experimental work or initial geometric morphometric analysis, GM analyses could and should be coupled with univariate analyses of linear data extracted from the landmark coordinates.

ACKNOWLEDGEMENTS

Data for this study were collected with permission from the American Museum of Natural History, the Department of Primatology at the State Collection of Anthropology and Paleoanatomy, the National Museum of Natural History, the Field Museum, and the Royal Museum for Central Africa. This manuscript was greatly improved by conversations with and comments from Bill Kimbel, Gary Schwartz, Mark Spencer, Chris Vinyard, Andrea Taylor, Janine Chalk, Erik Otárola-Castillo, Christine Wall, two anonymous reviewers, and associate editor Dallas Hyde.

LITERATURE CITED

Adams DC, Collyer ML. 2009. A general framework for the analysis of phenotypic trajectories in evolutionary studies. Evol 63:1143–1154.

Adams DC, Otárola-Castillo E. 2012. Package 'geomorph': Geometric morphometric analysis of 2d/3d landmark data. R package version 1.0.

Adams DC, Rohlf FJ. 2000. Ecological character displacement in *Plethodon*: biomechanical differences found from a geometric morphometric study. Proc Natl Acad Sci USA97:4106–4111.

Adams DC. 2004. Character displacement via aggressive interference in Appalachian salamanders. Ecol 85: 2664–2670.

Anderson MJ, Ter Braak CJF. 2003. Permutation tests for multifactorial analysis of variance. J Stat Comp Sim 73:85–113.

Anderson K, Throckmorton GS, Buschang PH, Hayasaki H. 2002. The effects of bolus hardness on masticatory kinematics. J Oral Rehabil 29:689–696.

Antón SC. 1996. Cranial adaptation to a high attrition diet in Japanese macaques. Int J Prim 17:401–427.

Baab KL, McNulty KP, Rohlf FJ. 2012. The shape of human evolution: a geometric morphometrics perspective. Evol Anthropol 21: 151–165.

Baab KL, McNulty KP. 2009. Size, shape, and asymmetry in fossil hominins: the status of the LB1 cranium based on 3D morphometric analyses. J Hum Evol 57:608–622.

Baab KL. 2008. The taxonomic implications of cranial shape variation in *Homo erectus*. J Hum Evol 54:827–847.

Badrian NL, Malenky RK. 1984. Feeding ecology of *Pan paniscus* in the Lomako Forest, Zaire. In: Susman RL, editor. The pygmy chimpanzee: evolutionary biology and behavior. New York: Plenum Press. p 275–299.

Bonnan MF. 2007. Linear and geometric morphometric analysis of long bone scaling patterns in Jurassic neosauropod dinosaurs: their functional and paleobiological implications. Anat Rec 290: 1089–1111.

Bookstein F, gunz P, Mitteroecker P, Prossinger H, Schaefer K, Seidler H. 2003. Cranial integration in *Homo*: singular warps analysis of the midsagittal plane in ontogeny and evolution. J Hum Evol 44:167–187.

Bookstein F, Schaefer K, Prossinger H, Seidler H, Fieder M, Stringer C, Weber GW, Arsuaga J-L, Rohlf FJ, Recheis W, Mariam AJ, Marcus LF. Comparing frontal cranial profiles in archaeic and modern *Homo* by morphometric analysis. Anat Rec 257:217–224.

Bouvier M. 1986a. A biomechanical analysis of mandibular scaling in Old World monkeys. Am J Phys Anthropol 69:473–482.

Bouvier M. 1986b. Biomechanical scaling of mandibular dimensions in New World monkeys. Int J Prim 7:551–567.

Brusatte SL, Sakamoto M, MOntanari S, Harcourt Smith WEH. 2012. The evolution of cranial form and function in theropod dinosaurs: insights from geometric morphometrics. J Evol Biol 25: 365–377.

Chapman C, White F, Wrangham R. 1994. Party size in chimpanzees and bonobos: a reevaluation of theory based on two similarly forested sites. In: Wrangham R, McGrew W, de Waal F, Heltne P, editors. Chimpanzee cultures. Cambridge: Harvard University Press. p 41–57.

Collyer ML, Adams DC. 2007. Analysis of two-state multivariate phenotypic change in ecological studies. Ecology 88:683–692.

Constantino PJ. 2007. Primate Masticatory Adaptations to Fracture-Resistant Foods. PhD Dissertation, George Washington University.

Daegling DJ, McGraw WS. 2001. Feeding, diet, and jaw form in West African *Colobus* and *Procolobus*. Int J Prim 22:1033–1055.

Daegling DJ. 1989. Biomechanics of cross-sectional size and shape in the hominoid mandibular corpus. Am J Phys Anthropol 80:91–106.

Daegling DJ. 2007. Relationship of bone utilization and biomechanical competence in hominoid mandibles. Arch Oral Biol 52:51–63.

Dumont ER. 1997. Cranial shape in fruit, nectar, and exudate feeders: implications for interpreting the fossil record. Am J Phys Anthropol 102:187–202.

Elgart-Berry A. 2004. Fracture toughness of mountain gorilla (*Gorilla gorilla beringei*) food plants. Am J Primatol 62:275–285.

Felsentein J. 1985. Phylogenies and the comparative method. Am Nat 125:1–15.

Fox EF, van Schaik CP, Sitompul A, Wright DN. 2004. Intra- and interpopulational differences in orangutan (*Pongo pygmaeus*) activity and diet: implications for the invention of tool use. Am J Phys Anthropol 125:162–174.

Greaves W. 1978. The jaw lever system in ungulates: A new model. J Zool Lond 184:271–285.

Gunz P, Bookstein FL, Mitteroecker P, Stadlmayr A, Seidler H, and Weber GW. 2009. Early modern human diversity suggests subdivided population structure and a complex out-of-Africa scenario. Proc Natl Acad Sci USA 106:6094–6098.

Harvati K. 2003. Quantitative analysis of Neanderthal temporal bone morphology using three-dimensional geometric morphometrics. Am J Phys Anthropol 120:323–338.

Hylander WL, Bays R. 1979. An in vivo strain-gauge analysis of the squamosal-dentary joint reaction force during mastication and incisal biting in *Macaca mulatta* and *Macaca fascicularis*. Arch Oral Bio 24:689–697.

Hylander WL, Johnson KR, Crompton AW. 1987. Loading patterns and jaw movements during mastication in *Macaca fascicularis*: a bone-strain, electromyographic, and Cineradiographic analysis. Am J Phys Anthropol 72:287–314.

Hylander WL. 1975. The human mandible: lever or link? Am J Phys Anthropol 43: 227–242.

Hylander WL. 1979. An experimental analysis of temporomandibular joint reaction force in macaques. Am J Phys Anthropol 51: 433–456.

Hylander WL. 1985. Mandibular function and biomechanical stress and scaling. Am Zool 25:315–330.

Hylander WL. 2006. Functional anatomy an biomechanics of the masticatory apparatus. In: Laskin JL, Greene CS, Hylander WL, editors. Temporomandibular disorders: an evidenced approach to diagnosis and treatment. New York: Quintessence Pub Co.

Jungers WL, Falsetti AB, Wall CE. 1995. Shape, relative size, and size-adjustments in morphometrics. Yearbk Phys Anthropol 38: 137–162.

Jungers WL. 1984. Aspects of size and scaling in primate biology with special reference to the locomotor skeleton. Yrbk Phys Anthropol 27:73–97.

Klingenberg CP, Gidaszewski NA. 2010. Testing and quantifying phylogenetic signals and homoplasy in morphometric data. Syst Biol 59:245–261.

Klingenberg CP, Bayaev AV, Sowry SM, Beckwith NJ. 2001. Inferring developmental modularity from morphological integration: analysis of individual variation and asymmetry in bumblebee wings. Am Nat 157:11–23.

Klingenberg CP. 2009. Morphometric integration and modularity in configurations of landmarks: tools for evaluating a priori hypotheses. Evol Devel 11:405–421.

Klingenberg CP. 2011. MorphoJ: an integrated software package for geometric morphometrics. Mol Ecol Res 11:353–357.

Komiyama O, Asano T, Suzuki H, Kawara M, Wada M, Kobayashi K, Ohtake S. 2003. Mandibular condyle movement during mastication of foods. J Oral Rehab 30:592–600.

Krogman WM. 1931a. Studies in growth changes in the skull and face of anthropoids. III. Growth changes in the skull and face of the gorilla. Am J Anat 47:89–115.

Krogman WM. 1931b. Studies in growth changes in the skull and face of anthropoids. IV. Growth changes in the skull and face of the chimpanzee. Am J Anat 47:325–342.

Lambert JE. 1999. Seed handling in chimpanzees (*Pan troglodytes*) and redtail monkeys (*Cercopithecus ascanius*): implications for understanding hominoid and cercopithecine fruit-processing strategies and seed dispersal. Am J Phys Anthropol 109:365–386.

Lewton KL. 2012. Evolvability of the primate pelvic girdle. Evol Biol 39:126–139.

Lockwood CA, Kimbel WH, Lynch JM. 2004. Morphometrics and hominoid phylogeny: Support for a chimpanzee-human clade and differentiation among great ape subspecies. Proc Natl Acad Sci USA 101:4356–4360.

Lockwood CA, Lynch JM, Kimbel WH. 2002. Quantifying temporal bone morphology of great apes and humans: an approach using geometric morphometrics. J Anat 201:447–464.

Lucas PW, Peters CR, Arrandale SR. 1994. Seed-breaking forces exerted by orang-utans with their teeth in captivity and a new technique for estimating forces produced in the wild. Am J Phys Anthropol 94:365–378.

Lynch JM, Wood CG, Luboga SA. 1996. Geometric morphometrics in primatology: craniofacial variation in *Homo sapiens* and *Pan troglodytes*. Folia Primatol 67:15–39.

Malenky RK, Wrangham RW. 1994. A quantitative comparison of terrestrial herbaceous food consumption by *Pan paniscus* in the Lomako Forest, Zaire, and *Pan troglodytes* in the Kibale Forest, Uganda. Am J Primatol 32:1–12.

McCollum MA. 2007. Rethinking incisor size and diet in anthropoids: diet, incisor wear and incisor breadth in the African apes. Am J Phys Anthropol 133:986–993.

McNulty KP, Frost SR, Strait DS. 2006. Examining affinities of the Taung child by developmental simulation. J Hum Evol 51:274–296.

Mitteroecker P, Gunz P, Bernhard M, Schaefer K, Bookstein FL. 2004. Comparison of cranial ontogenetic trajectories among great apes and humans. J Hum Evol 46:679–698.

Monteiro LR. 1999. Multivariate regression models and geometric morphometrics: the search for causal factors in the analysis of shape. System Biol 48:192–199.

Norconk MA, Wright BW, Conklin-Brittain NL, Vinyard CJ. 2009. Mechanical and nutritional properties of food as factors in platyrrhine dietary adaptations. In: Garber, PA, Estrada A, Bicca-Marques C, Heymann E, Strier K, editors. South American primates: testing new theories in the study of primate behavior, ecology, and conservation. New York: Springer Science. p 279–319.

Nunn CL, Barton RA. 2001. Comparative methods for studying primate adaptation and allometry. Evol Anthropol 10:81–98.

Nunn CL. 2011. The Comparative Method in Evolutionary Anthropology and Biology. Chicago: University of Chicago Press.

O'Higgins PO, Cobb SN, Fitton LC, Gröning F, Phillips R, Liu J, Fagan MJ. 2011. Combining geometric morphometrics and function simulation: an emerging toolkit for virtual functional analyses. J Anat 218:3–15.

O'Higgins P, Jones N. 1998. Facial growth in *Cercocebus torquatus*: an application of three dimensional geometric morphometric techniques to the study of morphological variation. J Anat 193:251–272.

Pierce SE, Angielczyk KD, Rayfield EJ. 2008. Patterns of morphospace occupation and mechanical performance in extant crocodilian skulls: a combined geometric morphometric and finite element modeling approach. J Morph 269:840–864.

Piras P, Colangelo P, Adams DC, Buscalioni A, Cubo J, Kotsakis T, Meloro C, Raia P. 2010. The Gavialis-Tomistoma debate: the contribution of skull ontogenetic allometry and growth trajectories to the study of crocodylian relationships. Evol Devel 12:568–579.

Ravosa MJ. 1990. Functional assessment of subfamily variation in maxillomandibular morphology among Old World monkeys. Am J Phys Anthropol 82:199–212.

Rice WR. 1989. Analyzing tables of statistical tests. Evolution 43: 223–225.

Rosas A, Bastir M. 2004. Geometric morphometric analysis of allometric variation in the mandibular morphology of the hominids of Atapuerca, Sima de los Huesos site. Anat Rec 278A:551–560.

Schultz AJ. 1969. The life of primates. New York: Universe.

Smith HF, Ritzman T, Otárola-Castillo E, Terhune CE. In press. A 3-D geometric morphometric study of intraspecific variation in the ontogeny of the temporal bone in modern *Homo sapiens*. J Hum Evol.

Smith HF, Terhune CE, Lockwood CA. 2007. Genetic, geographic, and environmental correlates of human temporal bone variation. Am J Phys Anthropol 134:312–322.

Smith HF. 2009. Which cranial regions reflect molecular distances reliably in humans? Evidence from three-dimensional morphology. Am J Hum Biol 21:36–47.

Smith RJ, Petersen CE, Gipe DP. 1983. Size and shape of the mandibular condyle in primates. J Morph 177:59–68.

Smith RJ. 1978. Mandibular biomechanics and temporomandibular joint function in primates. Am J Phys Anthropol 49:341–349.

Smith RJ. 1993. Categories of allometry: body size versus biomechanics. J Hum Evol 24:173–182.

Smith RJ. 2005. Relative size versus controlling for size. Curr Anthropol 46:249–273.

Spencer MA, Spencer GS. 1993. MacMorph Data Acquisition Package. Stony Brook, NY.

Spencer MA. 1998. Force production in the primate masticatory system: electromyographic tests of biomechanical hypotheses. J Hum Evol 34:25–54.

Spencer MA. 1995. Masticatory System Configuration and Diet in Anthropoid Primates. PhD Dissertation, State University of New York at Stony Brook.

Taylor AB, Vogel ER, Dominy NJ. 2008. Food material properties and mandibular load resistance abilities in large-bodied hominoids. J Hum Evol 55: 604–616.

Taylor AB. 2002. Masticatory form and function in the African apes. Am J Phys Anthropol 117:133–156.

Taylor AB. 2005. A comparative analysis of temporomandibular joint morphology in the African apes. J Hum Evol 48:555–574.

Taylor AB. 2006. Feeding behavior, diet, and the functional consequences of jaw form in orangutans, with implications for the evolution of *Pongo*. J Hum Evol 50:377–393.

Taylor AB. 2006. Feeding behavior, diet, and the functional consequences of jaw form in orangutans, with implications for the evolution of *Pongo*. J Hum Evol 50:377–393.

Terhune CE, Kimbel WH, Lockwood CA. 2007. Variation and diversity in *Homo erectus*: a 3D geometric morphometric analysis of the temporal bone. J Hum Evol 53:41–60.

Terhune CE. 2010. The Temporomandibular Joint in Anthropoid Primates; Functional, Allometric, and Phylogenetic Influences. PhD Dissertation, Arizona State University.

Terhune CE. 2011. Modeling the biomechanics of articular eminence function in anthropoid primates. J Anat 219:551–564.

Terhune CE. 2013. Dietary correlates of temporomandibular joint morphology in the great apes. Am J Phys Anthropol 150:260–272.

Tutin CEG, Fernandez M. 1993. Composition of the diet of chimpanzees and comparisons with that of sympatric lowland gorillas in the Lope Reserve, Gabon. Am J Primatol 30:195–211.

Ungar PS. 1994. Patterns of ingestive behavior and anterior tooth use differences in sympatric anthropoid primates. Am J Phys Anthropol 95:197–219.

Viðarsdottir US, O'Higgins P, Stringer C. 2002. A geometric morphometric study of regional differences in the ontogeny of the modern human facial skeleton. J Anat 201:211–229.

Vinyard CJ, Hanna J. 2005. Molar scaling in strepsirrhine primates. J Hum Evol 49:241–269.

Vinyard CJ, Wall CE, Williams SH, Hylander WL. 2003. Comparative functional analysis of skull morphology of tree-gouging primates. Am J Phys Anthropol 120:153–170.

Vinyard CJ. 2008. Putting shape to work: making functional interpretations of masticatory apparatus shapes in primates. In: Vinyard CJ, Ravosa MJ, Wall CE, editors. Primate craniofacial function and biology. New York: Springer Science. p 357–386.

Vinyard C. 1999. Temporomandibular Joint Morphology and Function in Strepsirrhine and Eocene Primates. PhD Dissertation, Northwestern University.

Vogel ER, van Woerden JT, Lucas PW, Atmoko SSU, van Schaik CP, Dominy NJ. 2008. Functional ecology and evolution of hominoid molar enamel thickness: *Pan troglodytes schweinfurthii* and *Pongo pygmaeus wurmbii*. J Hum Evol 55:60–74.

von Cramon-Taubadel N, Smith HF. 2012. The relative congruence of cranial and genetic estimates of hominoid taxon relationships: implications for the reconstruction of hominin phylogeny. J Hum Evol 62:640–653.

Wall C, Vinyard C, Johnson K, Williams S, Hylander W. 2006. Phase II jaw movements and masseter muscle activity during chewing in *Papio anubis*. Am J Phys Anthropol 129:215–224.

Wall CE. 1995. Form and Function of the Temporomandibular Joint in Anthropoid Primates, PhD Dissertation, State University of New York at Stony Brook.

Wall CE. 1997. The expanded mandibular condyle of the Megaladapidae. Am J Phys Anthropol 103:263–276.

Wall CE. 1999. A model of temporomandibular joint function in anthropoid primates based on condylar movements during mastication. Am J Phys Anthropol 109:67–88.

Watts DP. 1984. Composition and variability of mountain gorilla diets in the Central Virungas. Am J Primatol 7:323–356.

Williamson EA, Tutin CEG, Rogers ME, Fernandez M. 1990. Composition of the diet of lowland gorillas at Lope in Gabon. Am J Primatol 21:265–277.

Zelditch ML, Swiderski DL, Sheets HD, Fink WL. 2004. Geometric morphometric for biologists: a primer. London: Elsevier Academic Press.